

Modular Robot Wear for Walking Assistance According to Physical Functionality

Kunihiro Ogata¹, Toshiki Futawatari^{1,2}, Masahiro Fujimoto¹, Yumeko Imamura¹ and Yoshio Matsumoto^{1,3}

Abstract—As people age, walking can become difficult. This difficulty in walking can lead to further physical decline and eventually result in the need for caregiving. To prevent this, wearable robots supporting walking rehabilitation have been developed. In this study, we aim to develop a modular robot wear that can be customized according to the user's needs. The modular robot wear consists of motor modules, sensor modules, and a processor. Motor modules can be attached to any part of the body that requires assistance, enabling support not only in the sagittal plane but also in the frontal plane. By calculating the relative movement of the center of gravity based on the information from the acceleration sensors in the sensor modules, commands to the motor modules are generated. This allows for assistance tailored to the user's walking pattern. Through verification experiments of the robot wear's operation, we confirmed its ability to provide support according to changes in walking patterns. However, while the robot wear can induce changes in walking patterns, there are challenges regarding the output it provides to the wearer.

I. INTRODUCTON

Walking is important for independent daily living, but with aging, there can be a decline in physical function that makes walking difficult. In particular, conditions such as knee osteoarthritis (KOA) and osteoporosis can lead to difficulty walking due to decreased function of the musculoskeletal system, including joints and bones. This is referred to as locomotive syndrome, which is commonly observed in adults aged 40 and older [1]. Li et al. reported that falls mostly occur during walking [2]. Elderly individuals are at a higher risk of fracturing their pelvis by falling. Such fractures can lead to further immobilization, accelerating dependency and ultimately requiring care. Therefore, to reduce the increase in the care level required for the elderly, assistance with walking becomes crucial. Canes and walkers are major assistive devices for walking among the elderly. In particular, the RT.2 developed by RT.WORKS enables assistance on inclines and not only enhances the safety of walking but also extends the range of mobility [3]. However, it's worth noting that canes and walkers may limit hand movements, potentially increasing the risk of falls [4].

Therefore, there is increasing attention on walking assistance through wearable devices [5][6]. As a wearable robot aimed at rehabilitation, CyberDyne's HAL is notable [6].

¹Human Augmentation Research Center, National Institute of Advanced Industrial Science and Technology (AIST), 6-2-3 Kashiwa-no-ha, Kashiwa-shi, Chiba, Japan [ogata.kunihiro](mailto:ogata.kunihiro@nii.ac.jp), [futawatari-toshiki1002](mailto:futawatari-toshiki1002@aist.go.jp), [masahiro-fujimoto](mailto:masahiro-fujimoto@nii.ac.jp), [yumeko.imamura](mailto:yumeko.imamura@nii.ac.jp), yoshio.matsumoto@aist.go.jp

² Department of Human and Engineered Environmental Studies, GSFS, The University of Tokyo, 6-2-3 Kashiwa-no-ha, Kashiwa-shi, Chiba, Japan

³ Tokyo University of Science

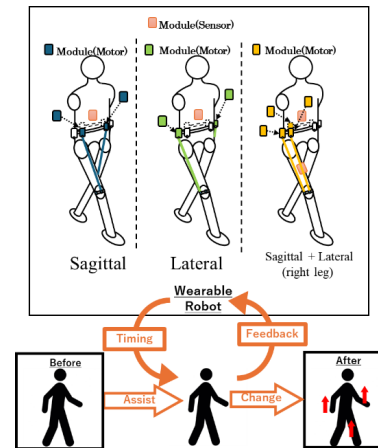


Fig. 1. Overview of modular robot wear.

Additionally, devices like Hocoma's Lokomat [7] and Toyota's Welwalk [8], which combine treadmills and displays to enhance rehabilitation effects, are gaining prominence. These robots consist of rigid hardware and are referred to as exoskeleton robots. Many conventional exoskeleton robots are limited to sagittal plane support. Kuo et al. argue that while sagittal plane movement is passively stabilized, stability in the frontal plane is maintained actively through control [9]. Consequently, exoskeleton robots capable of supporting both the sagittal and frontal planes are also being developed.

However, many patients may only have partial dysfunction in their lower limbs, such as stroke patient, making exoskeleton robots like those mentioned above functionally redundant. There are few examples of wearable robots that can provide tailored support according to each user's individual physical function.

II. PROPOSAL AND PURPOSE

In this study, we aim to develop wearable robots capable of providing support tailored to the user's conditions and challenges. To achieve this, it is necessary to decompose the functions of the robot and reconfigure them for each user. Therefore, we propose a modular wearable robot.

A. Proposed Robot

The concept of modular robot wear is illustrated in Fig. 1. This robot wear modularizes functions such as actuators, sensors, processors, etc., allowing these modules to be attached in the required numbers to the necessary areas. For example, if support is needed in the sagittal plane of both legs, actuators would be attached to the anterior surface of

both thighs as shown on the left side of Fig. 1. If support is needed in the frontal plane, actuators would only be attached to the sides of the thighs as shown in the center of Fig. 1. In the case of patients with hemiplegia where only one leg is affected, actuators would be attached to the front, side, and back of the affected leg (shown on the right side of Fig. 1). This approach enables tailored support for each user, ensuring adequate assistance according to individual needs.

Furthermore, regarding sensing, if only center of gravity acceleration is sufficient, then attaching a single IMU (Inertial Measurement Unit) to the waist would be adequate. If trunk posture is required, IMUs can be added to the chest or back. If hip flexion-extension angles are necessary, IMUs can be added to the thighs. In this way, adjustments according to the specific requirements of sensing become feasible.

Conventional wearable robots can be broadly classified into two types: those that cover the wearer with a frame, known as the 'framed type,' and those that do not, known as the 'frameless type.' Examples of framed type include HAL [6] and ReWalk [5]. An example of frameless type is HIMICO by ATOUN [10]. While framed types typically offer greater output, they are considered challenging to modularize. On the other hand, frameless types provide lower output to the wearer but are thought to be easier to modularize. Therefore, in this study, we aim to develop a frameless-type wearable robot.

The frameless type, as mentioned earlier, has limitations in the output it provides to the wearer. Therefore, our objective is not to provide assistance through passive exercise with power assistance, but rather to induce active exercise by instructing the timing and direction of movement. The concept of support for inducing active exercise is illustrated in Fig. 1 (bottom). By providing force at any desired timing, we consciously alter the wearer's gait, prompting adjustments in stride length and center of gravity movement. In this way, by inducing active exercise, it becomes possible to train while leveraging the wearer's residual function, which is expected to lead to improvements in the quality of walking effectively.

There are several previous studies of research on modular wearable robots. Mejineke et al. have developed the wearable robots that can assist users with spinal cord injuries (SCI) in walking independently [11]. This robot has a removable hip, knee and ankle joint motors. However, only the sagittal plane is assumed. Xeloyannis et al. have developed the flexible wearable robots to assist upper limb [12]. Modularizing the wire drive mechanism makes it possible to provide the necessary support for both arms. Modularization to any part of the body has not been fully verified.

B. Purpose in this Study

The ultimate goal of this study is to achieve walking rehabilitation using the modular robot wear as described in the preceding sections. This paper aims to develop a prototype of the modular robot wear and verify its functionality. In the following chapters, we will discuss the hardware, control system, and verification experiments of the modular robot wear.

III. MODULAR ROBOT WEAR

This chapter discusses the hardware of the modular robot wear.

A. Actuator Arrangement

When correcting movements such as shifting the center of gravity or adjusting stride, it is believed to be effective to provide assistance to the hip joint. Therefore, actuators are positioned to support the hip joint. Figure 2 illustrates the arrangement of actuators.

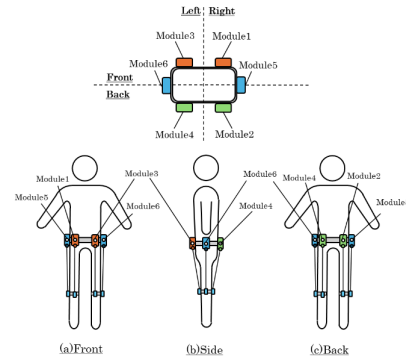


Fig. 2. Arrangement of motor modules.

Modules 1 and 3 are expected to widen the stride by attaching them to the front of the hip joint. Modules 2 and 4, when attached to the back of the hip joint, are expected to narrow the stride. Modules 5 and 6, when attached to the sides of the hip joint, are expected to alter the center of gravity shift left and right.

B. Motor Module

The motor modules need to be attachable to any part of the body and capable of providing force presentation. Therefore, in this study, cable-driven actuation is adopted for the motor modules. This allows for individual adjustments based on body characteristics through the length of the cables.

As mentioned earlier, this study primarily aims to support the hip joint. When the hip joint flexes, the cables of modules 1 and 3 in Fig. 2 tend to loosen, while the cables of modules 2 and 4 are pulled strongly due to the significant deformation of the buttocks. These factors pose significant challenges for force presentation. To address the slackening and tensioning of cables caused by joint movements, it is necessary to control the length of the cables appropriately.

One possible method to adjust the tension of the cables caused by hip joint movement is through torque control of the motors. Since real-time control of multiple actuators is required in this robot wear, a simple control method is desirable. Therefore, by attaching rubber to the end of the cables and utilizing the expansion and contraction of the rubber, changes in the cables due to movement can be absorbed. Then, at times when force needs to be applied, the motors can pull the cables to provide tension. The tension provided can be adjusted by the length of the cables (position control), which is convenient. Figure 3 shows the appearance of the motor modules fabricated in this study.

A Kondo Kagaku servo motor (B3M-1170-A) was used. This servo motor is compact yet capable of generating output up to 7.8 Nm, sufficient to provide the required tension for force presentation. Tension can be obtained by winding the cables through pulleys driven by the motors. For the rubber part, Esco's plain weave rubber (EA628PV-162, width 50mm) was used.

The tension provided varies depending on the spring constant of the rubber. The spring constant of the rubber depends on its length. Therefore, we examined the relationship between the length of the rubber and its spring constant. Various lengths of rubber were prepared, and the tension was measured when stretched to a certain length. For measurements, we utilized a six-axis force sensor manufactured by Leprino Corporation (FFS055YA501U6). The appearance of the measuring device and the experimental results are shown in Fig. 4(a).

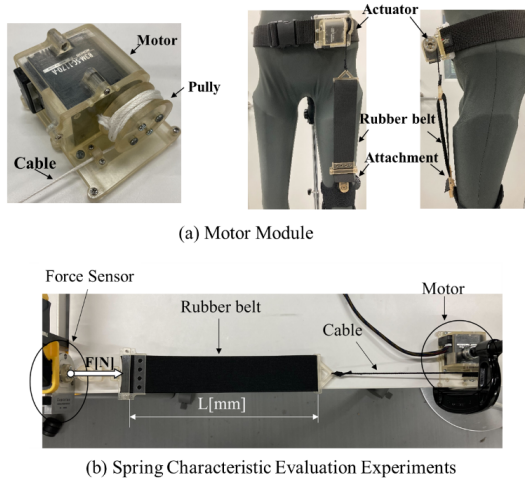


Fig. 3. (a) Appearance of developed motor module. (b) Performance testing of the motor module.

From previous studies [13], it is known that the spring constant and elongation ratio of rubber are nonlinear. Based on experimental data, we identified a model equation for the spring constant. The calculated model equation is $k = 48.137 \times L^{-0.815}$, where k represents the spring constant and L represents the elongation of the rubber. The correlation between the spring constant obtained from this equation and the actual spring constant is 0.990, suggesting that appropriate spring constants can be obtained using this model equation.

Next, the time response was examined utilizing the apparatus depicted in Fig. 3(b). The peak timing of tension was measured as the cable was wound to different lengths. The experimental results are shown in Fig. 4(b). In this experiment, the length of the rubber was set to 200mm. The winding lengths were set to 10mm, 20mm, 30mm, 40mm, and 50mm. As the target winding length decreases, the peak timing occurs earlier. At 10mm, it occurs approximately 0.25 seconds after winding, while at 50mm, it occurs around 0.9 seconds. Here, the average comfortable walking cycle for a person in their 20s is approximately 1.1 seconds [14], with

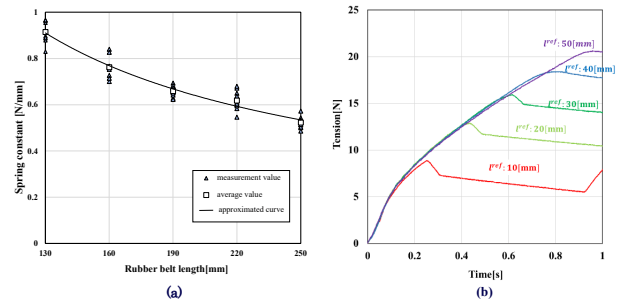


Fig. 4. (a) Measurement results of the spring constant. (b) Measurement results of the response time.

each step taking around 0.55 seconds. This implies that the peak should be reached in 0.55 seconds or less. To ensure that force presentation can be provided within one step and to deliver greater tension, a target winding length of 20mm seems reasonable.

C. Sensor Module

Observing the state during walking requires one or more sensors. Examples of sensors include IMUs capable of acquiring acceleration and angular velocity during walking, as well as pressure sensors capable of detecting the contact status between the feet and the environment. These sensors need to be appropriately selected based on the purpose and the wearer's condition.

In this study, a single IMU was used as the minimal configuration for estimating the wearer's walking state. While using multiple sensors is desirable for obtaining high estimation accuracy, this study aimed to estimate the wearer's state with the minimal number of sensors. To estimate the wearer's state using a single IMU, it is preferable to attach the IMU to the trunk. Literature [15] has shown that estimating walking state by attaching an IMU to the waist is feasible. Therefore, it is reasonable to attach the IMU to the waist when estimating walking state with a single IMU. The IMU used in this study is the InvenSense 9-axis sensor module MPU-9250. The information from this IMU is acquired by a microcontroller (mbedHRM1017r3) and transmitted to a PC.

D. Robot Wear

The appearance of the developed modular robot wear is shown in Fig. 5.

In Fig. 5(a), motors are attached to the waist and provide force presentation using a cable winding mechanism. Actuators are mounted on the front and back of the hip joint for sagittal plane support. Additionally, an IMU is attached to the back of the waist. Commands to the motors are computed based on sensor information using a PC. Future plans aim to operate using small embedded computers like Raspberry Pi. Furthermore, as shown in Fig. 5(b), it is also possible to laterally attach motors for frontal plane support. The same motors are used, and the configuration allows for the adjustment of mounting positions.



Fig. 5. The appearance of the developed modular robot wear. (a) Sagittal plane assist. (b) Frontal plane assist.

IV. CONTROL SYSTEM

The control system for presenting force sensations in real time based on the walking state of the wearer will be described.

In conventional robot wearables designed for walking assistance, the walking pattern of healthy individuals was taught based on the walking cycle [10]. With this approach, even when individuals are walking properly, they would still receive assistance, potentially hindering conscious improvement of their function. Therefore, in this study, a method is proposed to quantify walking function with an arbitrary parameter x_p and provide appropriate assistance when needed by providing feedback based on this parameter.

As mentioned in the previous chapter, multiple motor modules and a single IMU are attached to the waist. In this study, an algorithm is considered to instruct appropriate gait using this configuration. An overview of the control system is illustrated in Fig. 6. The quantification of walking function utilizes information obtained from the IMU. By providing walking parameters x_p obtained from the IMU and the desired walking parameters x_p^d to the controller, the corrective center of mass velocity \dot{x} is calculated. This center of mass velocity is distributed to each joint, and assistance is provided by driving the motor modules based on this distribution.

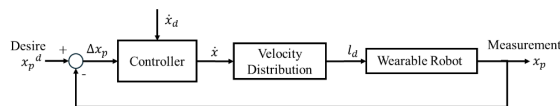


Fig. 6. Control block diagram of the robot wear.

A. Estimating Walking State

To control in real-time according to the wearer's walking, it is necessary to estimate the wearer's walking state. Methods have been proposed to estimate events such as heel strike

(HS), toe-off (TO), and stance phase. In this study, a method was developed to detect HS (stance leg change), determine the stance leg, and estimate the walking cycle by modeling human walking motion as an inverted pendulum.

In steady-state walking, the height of the center of mass reaches a maximum when it is directly above the supporting leg and a minimum at HS, after which it increases. When modeling the center of mass trajectory as a sine wave, it is observed that the second derivative of the center of mass acceleration reaches a maximum at HS. Mechanically, this signifies that the vertical acceleration reaches a maximum due to the kicking force applied to the ground during the swing phase. Based on this, the timing of HS is calculated using the vertical acceleration. The calculation flow is shown in Fig. 7(a). It is also possible to calculate the walking cycle based on the timing of HS.

Next, this section explains how to determine the support leg. During walking, the lateral acceleration in the left-right direction shifts according to the supporting leg. However, due to noise in the actual sensor values, it is challenging to determine left or right based on instantaneous acceleration values. Therefore, determining the lateral shift based on the velocity obtained by integrating the acceleration is proposed. When integrating the acceleration sensor, the calculation results may diverge due to drift errors, so the integration interval is set to one step. The timing of one step's data extraction is determined using the previously mentioned HS timing detection algorithm. However, when the sensor is attached to a person, it may shift to either the left or right, causing the calculation results to shift in either direction regardless of the supporting leg. Therefore, the average velocity obtained from several steps of data is used as a reference value to determine whether the center of mass is shifting to the left or right. This calculation flow is illustrated in Fig. 7(b).

B. Controller based on COG-ZMP Model

Humanoid robots utilize control methods based on the Zero Moment Point (ZMP) as a representative point for the contact force between the robot and the environment in achieving walking motions [16]. This information is employed for stabilizing the robot and preventing falls, making it suitable for obtaining the overall state of walking. The ZMP is obtained from the center of mass position and center of mass acceleration using Eq. (1). It's worth noting that both the x-axis and y-axis directions follow the same equation, so only the x-axis direction is illustrated here.

$$x_z = x_m - \frac{\ddot{x}_m}{\ddot{z}_m + g} z_m \quad (1)$$

$$x_m - x_z = \frac{\ddot{x}_m}{\ddot{z}_m + g} z_m$$

$$x_p = \frac{\ddot{x}_m}{g} z_c \quad (2)$$

Where, the center of mass coordinates are denoted as (x_m, z_m) , the ZMP is represented as x_z , and g stands for the gravitational acceleration. By combining the center of

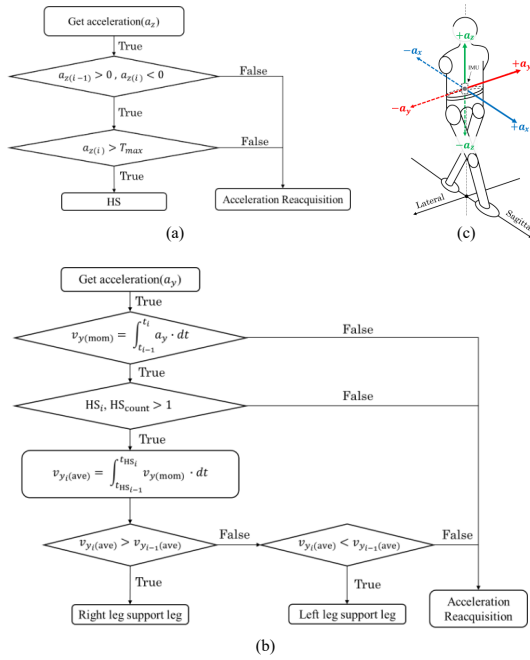


Fig. 7. (a) HS detection algorithm. (b) Support leg determination algorithm. (c) Coordinate system.

mass position x_m and the ZMP x_z on the left side, and using the approximation $\ddot{z}_m \simeq 0$, since the change in acceleration along the vertical axis is small compared to the gravitational acceleration, Eq. (2) is obtained. The physical quantity x_p obtained from this equation represents the relative position of the center of mass with respect to the ZMP, termed as the relative center of mass displacement. Here, z_c denotes the average center of mass height. Since this relative center of mass displacement is derived from the center of mass acceleration, it can be calculated from the IMU attached to the waist. x_p is utilized as a walking parameter in Fig. 6 for controlling the robot ware.

By utilizing the center of mass position and ZMP as feedback, stability control of humanoid robots has been achieved. In this study, the method of Choi et al. is applied to the relative center of mass displacement [17]. The control input is represented by Eq. (4).

$$\dot{x} = u + e \quad (3)$$

$$\dot{x} = \dot{x}^d + k_g (x_p^d - x_p) + e \quad (4)$$

Where, u represents the control input, e is the disturbance term, \dot{x}^d denotes the target center of mass velocity, and k_g is the control gain. The obtained center of mass velocity from this equation is then distributed to the joints to determine the commands for the motors.

The distribution of center of mass velocity can be achieved using techniques such as resolved momentum control [16]. In this study, focusing on the movement of the hip joint in the frontal or sagittal plane, the wearer is simplified as a one-degree-of-freedom model to distribute the center of mass velocity. The center of mass position can be obtained from the foot length l and the hip joint angle θ using the following

equation. By differentiating this equation, the relationship between the center of mass velocity and the joint angular velocity can be derived.

$$x = l \sin \theta \quad (5)$$

$$\dot{x} = l \cos \theta \dot{\theta} \quad (6)$$

$$l_d = k_\theta \frac{\dot{x}}{l \cos \theta}$$

Where, k_θ represents the control gain related to the winding length. By multiplying the joint angular velocity obtained from the above equation by an arbitrary gain, the length of the cable winding can be determined.

Thus, it becomes possible to control the length of the cable winding of the motor modules by providing feedback of the relative center of mass displacement calculated from the IMU.

V. EXPERIMENTS

The developed robot wear was subjected to evaluation experiments. Firstly, the real-time control in accordance with human walking was verified(V-A). This involved testing the placement of motor modules for sagittal plane support and frontal plane support. Subsequently, the wearable robot was worn, and verification was conducted to ascertain whether the wearer's gait changed while walking(V-B). This research received approval from the Life Science Committee of the National Institute of Advanced Industrial Science and Technology (AIST) (ID: 2022-1247).

A. Operation Verification Experiments

1) *Purpose*: The aim of this robot wear is to provide assistance based on the wearer's gait. In this experiment, the objective is to verify whether the robot wear responds accordingly when the wearer changes their gait.

2) *Conditions*: In this experiment, one healthy male participant in his twenties wore two patterns of the robot wear to assess how its behavior changes in response to alterations in gait. Pattern 1 provided support in the sagittal plane(Fig. 5(a)), while Pattern 2 provided support on the frontal plane(Fig. 5(b)). In Pattern 1 experiments, the participant was asked to walk with various step stride to verify if the robot wear's control system could adapt to changes in step stride. Similarly, in Pattern 2 experiments, the participant varied step width. For a typical male in his twenties, the average step stride is 0.75 meters, and the step width is 0.10 meters. These values were measured beforehand to establish the target state, and the average relative position of the center of mass at that state was used for control.

The participant was instructed to walk according to marks placed on the floor. For the verification experiments of Pattern 1, two types of step strides, 0.5m and 1.0m, were prepared. Since the target step stride was 0.75, the robot wear was driven to widen the step stride if it was narrower than 0.75 and to narrow it if it was wider. In the experiments for Pattern 2, two types of step widths, 0.10m and 0.30m, were prepared. Since the target step width was 0.10, the robot wear was driven to narrow the step width if it was wider than 0.10.

In both experiments, the participant walked approximately 30 meters. Changes in the participant's gait were measured using an inertial motion capture system (Movella Awinda).

3) *Results and Discussion:* The experimental results are presented in Figs. 8 and 9. Figure 8 depicts the hip joint angle in the Pitch axis and the cable winding length during assist in Pattern 1. It is observed that the hip joint angle varies between narrow and wide stride intervals. Furthermore, it is evident that Modules 1 and 3 motor modules are active during narrow stride intervals. Modules 1 and 3, mounted at the front, are expected to assist in hip flexion when activated. On the other hand, Modules 2 and 4 motor modules are active during wide stride intervals. Modules 2 and 4, attached at the rear, are expected to restrain hip flexion when activated.

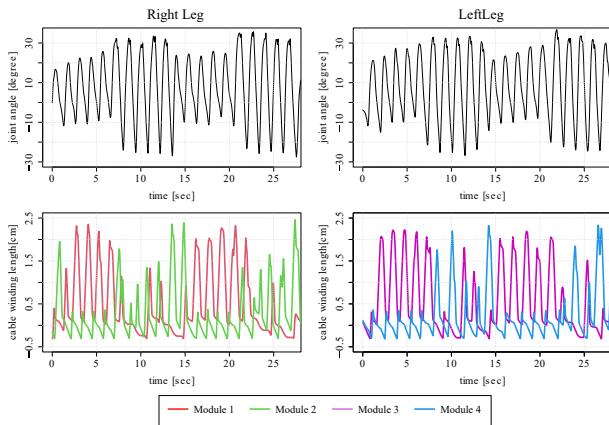


Fig. 8. Experimental results of sagittal plane assist. Hip joint angles and cable winding length.

Figure 9 shows the hip joint angle in the Roll axis and the cable winding length during support in Pattern 2. In the interval with a step width of 0.10, the variation in hip joint angle is small, but it becomes pronounced when the step width increases to 0.30. Correspondingly, it is observed that the winding length increases. Although there are some regions with shorter winding lengths, it is evident that the system is capable of providing suitable assistance in response to changes in step width.

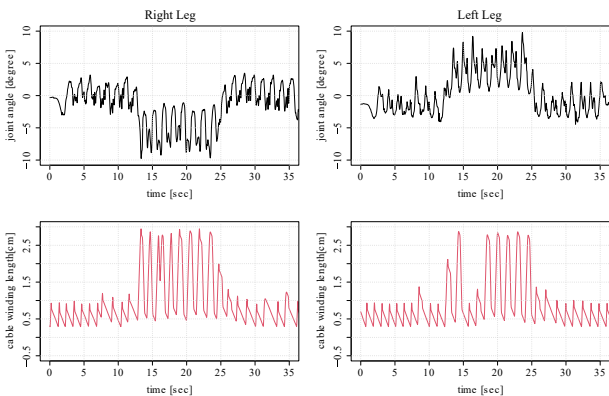


Fig. 9. Experimental results of frontal plane assist. Hip joint angles and cable winding length.

B. Verification Experiments on Changes in Wearer's Gait

1) *Purpose:* The previous section confirmed that the developed robot wear can be appropriately controlled to match the wearer's gait. In this experiment, the basic goal is to verify whether the robot wear can alter the wearer's gait.

2) *Conditions:* Three healthy male participants in their 20s (A, B, C) were recruited for the experiment. To maintain a consistent walking pace, participants were instructed to walk to the sound of a metronome during the experiment. The tempo of the metronome was set to 100 beats per minute (corresponding to approximately 0.6 seconds between HS). Changes in the participants' gait were measured using an inertial motion capture system (Awinda by Movella). This experiment focused on the Pattern 1 of the robot wear as described in the previous section.

Before conducting the experiment, participants were asked to walk naturally for a distance of 20 meters while wearing the robot wear. This allowed measurement of the average changes in the participants' relative center of mass. Additionally, while in a static position, the length of the cables from the motor modules was adjusted, setting the initial length to the maximum winding length where the wearer did not feel any force from the wear. At the same time, it was ensured that the wearer could feel the force when the cables were wound by 0.02 meters.

Four types of experiments were conducted: no support, support only on the right leg, support only on the left leg, and support on both legs. The support provided by the robot wear was confined to the sagittal plane. The target values provided by the robot wear were set to two types: adding 0.15 meters to the standard relative center of mass displacement and subtracting 0.15 meters from it. These target values were not communicated to the wearers and were randomly assigned.

3) *Results and Discussion:* The experiment participants were instructed to specify their stride for the first five steps and then to follow the force presentation from the sixth step onwards. Therefore, the change in hip angle from the first five steps was used as the evaluation metric. The experimental results are presented in Fig. 10 and Table I.

Figure 10 depicts the changes in hip angle for participant A during each step when only the right leg was supported. The left side of the figure represents the results without assistance, while the right side shows the results with assistance. As evident from Fig. 10, while no significant changes were observed in the left leg, cases were observed where the hip angle of the right leg increased with assistance.

Next, a statistical analysis of the changes in hip angle was conducted for each participant. Since there were no significant differences observed among the data of the three participants, only the data from one participant are presented in this paper. Table I shows the results of the significance test between the unsupported and supported conditions for participant B. The evaluation metric used was the change in hip angle.

In the case of "Target value = 0.60", a significant increase in step stride was observed, indicating that the intended outcome was achieved. However, the change in hip angle

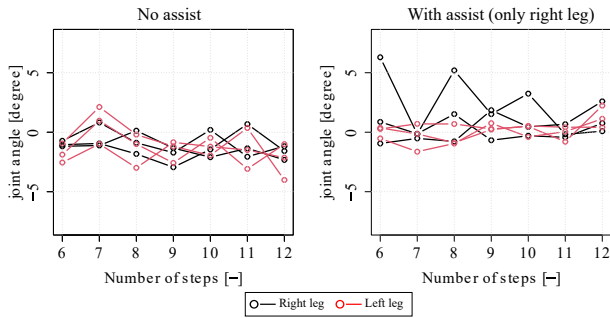


Fig. 10. Experimental results of right leg assist. Changes in hip joint angle per step.

was not very pronounced. This suggests that a reassessment of the magnitude of force applied to the wearer is necessary.

On the other hand, in the case of "Target value = 0.30", the expected decrease in step stride was not observed. This may indicate that the magnitude or timing of the force applied to reduce hip angle was not appropriate, suggesting room for improvement in the motor module.

TABLE I

RESULTS OF THE STATISTICAL ANALYSIS ON THE CHANGES IN HIP JOINT ANGLES.

	0.60m		0.30m	
	Average [°]	p-value	Average [°]	p-value
Right leg assist				
Right leg	1.68	0.00214	0.505	0.00322
Left leg	-0.105	0.209	-1.39	0.0286
Left leg assist				
Right leg	1.18	1.02×10^{-5}	0.416	0.00533
Left leg	0.676	0.0215	1.99	0.00114
Both leg assist				
Right leg	1.06	0.000169	-1.42	0.471
Left leg	0.869	0.0142	0.734	0.0103

VI. CONCLUSION

Physical impairments vary among users, necessitating tailored support for each individual. Therefore, in this study, a modular robotic exosuit that allows for customizable configurations based on the user's needs was developed. The developed modular exosuit consists of motor modules, sensor modules, and a computing unit.

The motor modules are composed of servo motors, pulleys, cables, and rubber. By varying the stiffness of the cables wound around the pulleys with rubber, force presentation is provided. As for sensor modules, IMUs are adopted. Although using multiple sensor modules is possible, in this study, a single IMU is used as the minimum configuration to estimate walking events and calculate walking function indicators (relative center of mass displacement), which are then used for robot control.

Human walking is formalized using the center of mass ZMP model, enabling real-time force presentation by utilizing relative center of mass displacement as feedback. Evaluation experiments confirmed that the motor modules change

commands and the cable winding length varies according to the walking state. However, evaluation experiments with multiple participants revealed insufficient force presentation, indicating the need for improvements in the robot wear.

In the future, we plan to improve the force presentation of the motor modules by modifying servo motors and revising control algorithms. Additionally, we will collaborate with physical therapists to discuss specific usage scenarios in real-world environments.

ACKNOWLEDGMENT

We express our heartfelt gratitude to Dr. Akihiko Murai and Miss Tianyi Zhu for their invaluable contributions to this research.

REFERENCES

- [1] Kozo Nakamura, Locomotive Syndrome : The Concept and Recent Topics, The Japanese Journal of Rehabilitation Medicine, Vol. 13, No. 12, pp. 890-893, 2016.
- [2] W. Li, T. HM Keegan, B. Sternfeld, S. Sidney, C. P. Quesenberry Jr, and J. L. Kelsey. Outdoor falls among middle-aged and older adults: a neglected public health problem. American journal of public health, Vol. 96, No. 7, pp. 1192-1200, 2006.
- [3] RT.WORKS. Robot Assist Walker RT. 2, <https://www.rtworks.co.jp/>, last access data: 05th Jan, 2023.
- [4] W. C. Mann, C. Granger, D. Hurren, M. Tomita, and B. Charvat. An analysis of problems with canes encountered by elderly persons. Physical & Occupational Therapy in Geriatrics, Vol. 13, No. 1-2, pp. 25-49, 1995.
- [5] A. Esquenazi, M. Talaty, A. Packel and M. Saulino, "The ReWalk Powered Exoskeleton to Restore Ambulatory Function to Individuals with Thoracic-Level Motor-Complete Spinal Cord Injury," Am J Phys Med Rehabil. 2012 Nov;91(11):911-21.
- [6] T. Ogata, H. Abe, K. Samura, et al. Hybrid Assistive Limb (HAL) Rehabilitation in Patients with Acute Hemorrhagic Stroke. Neurol Med Chir (Tokyo), Vol. 55, No. 12, pp. 901-906, 2015. doi:10.2176/nmc.0a.2015-0209.
- [7] K. Y. Nam, H. J. Kim, B. S. Kwon, J. Park, H. J. Lee and A. Yoo, "Robot-assisted gait training (Lokomat) improves walking function and activity in people with spinal cord injury: a systematic review," Journal of NeuroEngineering and Rehabilitation volume 14, 24, 2017.
- [8] "Toyota Refines Rehabilitation Assist Robot and Launches New Well-walk WW-2000," November 21, 2019, Toyota Motor Corporation.
- [9] A. D. Kuo : "The six determinants of gait and the inverted pendulum analogy: A dynamic walking perspective" Human movement science, vol. 26, no.4, pp. 617-656, 2007.
- [10] F. Hiromichi, K. Kazuaki, "Development Report on the "HIMICO" Power Assist Suit for Walking Support," IATSS Review, 47(1) 40-47, Jun 30, 2022.
- [11] C. Meijneke, et al. "Symbitron Exoskeleton: Design, Control, and Evaluation of a Modular Exoskeleton for Incomplete and Complete Spinal Cord Injured Individuals." IEEE Trans Neural Syst Rehabil Eng. 29, pp.330-339, 2021.
- [12] M. Xiloyannis, et al. "Design and Validation of a Modular One-To-Many Actuator for a Soft Wearable Exosuit!" frontiers in Neuro-robotics, 18, 2019.
- [13] S. Miyamoto, T. Watanabe and A. Tomoda, "Behavior of the string considering axial elongation," Transactions of the JSME (in Japanese), vol. 82, no. 839, 2016.
- [14] M. Yamasaki, H. Sato, "Human walking: With reference to step length, cadence, speed and energy expenditure," Journal of the Anthropological Society of Nippon 98 (4), 385-401, 1990.
- [15] H. Lim, B. Kim, and S. Park. "Prediction of lower limb kinetics and kinematics during walking by a single IMU on the lower back using machine learning. Sensors, Vol.20, No.1, 2019.
- [16] S. Kajita, H. Hirukawa, K. Harada and K. Yokoi, "Introduction to Humanoid Robotics," Springer, 2014.
- [17] Y. Choi, D. Kim, Y. Oh and B.J. You. "Posture/walking control for humanoid robot based on kinematic resolution of Com jacobian with embedded motion," IEEE Transactions on Robotics, vol.23, pp.1285-1293, 2007.